IOSR Journal of Applied Physics (IOSR-JAP)
e-ISSN: 2278-4861.Volume 18, Issue 2 Ser. II (Mar – Apr 2026), PP 01-08
www.iosrjournals.org

Spectral, Thermal and Photoluminescence Analysis of Phosphate Glasses with Trivalent Holmium for 2.0µm optoelectronic applications

S.L. Meena
Ceramic Laboratory, Department of physics, Jai Narain Vyas University, Jodhpur 342001(Raj.) India

Abstract
Glasses samples containing Ho^{3+} in Ytterium Zinc Lithium Sodalime Magnesium Phosphate Glasses (45-x)P_2O_5: 10ZnO: 10Li_2O: 10Na_2O: 15CaO: 10MgO: 10Y_2O_3 :xHo_2O_3 (where x=1, 1.5,2 mol %) have been prepared by melt-quenching method. The amorphous nature of the prepared glass samples was confirmed by X-ray diffraction. DTA curve was analysed to evaluate the glass transition temperature, crystallization temperature and melting temperature Optical absorption, Excitation and fluorescence spectra were recorded at room temperature for all glass samples. Judd-Ofelt intensity parameters Ω_λ (λ=2, 4 and 6) are evaluated from the intensities of various absorption bands of optical absorption spectra. Using these intensity parameters various radiative properties like spontaneous emission probability (A), branching ratio (β), radiative life time (τ_R) and stimulated emission cross–section (σ_p) of various emission lines have been evaluated.

Keywords: *YZLSLMP Glasses, Thermal Properties, Judd-Ofelt Theory, Luminescence Analysis.*

I. Introduction

Rare earth glasses are important materials which find new opportunities in the field of optical fiber amplifiers, up-conversion lasers, waveguide laser, electro-luminescent devices, memory devices optical fibers, sensors, glass lasers [1–5].Among different glasses phosphate glasses have unique properties. They have high refractive index, low dispersion rates, high transparency, good chemical and thermal stability, Phosphate glasses are thermally and chemically stable besides transparent at the emission and excitation wavelengths [6-8].The photoluminescence properties of phosphate glasses is also compressed because of their relatively large phonon energy. Phosphate glasses can be a good matrix for fiber lasers because they exhibit good mechanical property. Phosphate glasses are both scientifically and technologically important materials because they generally offer some unique sprctral, thermal and physical properties better than other glasses [9-12].

The addition of network modifier B_2O_3 is to improve mechanical strength and thermal stability. Zinc oxide is added in the glass matrix to increase glass forming ability and to ensure low rates of crystallization in the glass system. Among active rare-earth ions Ho^{3+} exhibits high solubility in ceramic glasses, which also possess excellent physical, optical and Thermal properties [13-15]. Recently phosphate based glasses have a wide range of potential applications in thermal photonic,laser action optical data transmission applications [16-18].

The present work reports on the preparation and characterization of rare earth doped heavy metal oxide (HMO) glass systems for lasing materials. I have studied on the Optical absorption, Excitation and fluorescence spectra of Ho^{3+} doped ytterium zinc lithium sodalime magnesium phosphate glasses. The thermal parameter like), Balaji Parameter (B_P), Hurbe's criterion (H_R) and Shankar's parameter (K_S) are calculated using DTA curve. The intensities of the transitions for the rare earth ions have been estimated successfully using the Judd-Ofelt theory, The laser parameters such as radiative probabilities(A),branching ratio (β), radiative life time(τ_R) and stimulated emission cross section(σ_p) are evaluated with the help of luminescence spectra.

II. Experimental Techniques

Preparation of glasses

The following Ho^{3+}doped phosphate glass samples (45-x)P_2O_5: 10ZnO: 10Li_2O: 10Na_2O: 15CaO: 10MgO: 10Y_2O_3 :xHo_2O_3. (where x=1,1.5 and 2 mol%) have been prepared by melt-quenching method. Analytical reagent grade chemical used in the present study consist of P_2O_5, ZnO, Li_2O, Na_2O, CaO, MgO,Y_2O_3 and Ho_2O_3. They were thoroughly mixed by using an agate pestle mortar. then melted at 1060^0C by an electrical muffle furnace for 2h., After complete melting, the melts were quickly poured in to a preheated stainless steel mould and annealed at temperature of 250^0C for 2h to remove thermal strains and stresses. Every time fine powder of cerium oxide was used for polishing the samples. The glass samples so prepared were of good optical

quality and were transparent. The chemical compositions of the glasses with the name of samples are summarized in **Table 1.**

Table 1.

Chemical composition of the glasses

Sample	Glass composition (mol %)
YZLSLMP (UD)	$45P_2O_5$: 10ZnO: $10Li_2O$: $10Na_2O$: 15CaO: 10MgO: $10Y_2O_3$
YZLSLMP HO (1.0)	$44P_2O_5$: 10ZnO: $10Li_2O$: $10Na_2O$: 15CaO: 10MgO: $10Y_2O_3$:$1Ho_2O_3$
YZLSLMP HO (1.5)	$43.5P_2O_5$: 10ZnO: $10Li_2O$: $10Na_2O$: 15CaO: 10MgO: $10Y_2O_3$:1.5 Ho_2O_3
YZLSLMP HO (2.0)	$43P_2O_5$: 10ZnO: $10Li_2O$: $10Na_2O$: 15CaO: 10MgO: $10Y_2O_3$:2 Ho_2O_3

YZLSLMP (UD) -Represents undoped Ytterium Zinc Lithium Sodalime Magnesium Phosphate glass specimen.
YZLSLMP (HO)-Represents Ho^{3+} doped Ytterium Zinc Lithium Sodalime Magnesium Phosphate glass specimens.

III. Theory

3.1 Oscillator Strength

The intensity of spectral lines are expressed in terms of oscillator strengths using the relation [19].

$$f_{expt.} = 4.318 \times 10^{-9} \int \varepsilon(\nu)\, d\nu \qquad (1)$$

where, $\varepsilon(\nu)$ is molar absorption coefficient at a given energy ν (cm^{-1}), to be evaluated from Beer–Lambert law. Under Gaussian Approximation, using Beer–Lambert law, the observed oscillator strengths of the absorption bands have been experimentally calculated [20], using the modified relation:

$$P_m = 4.6 \times 10^{-9} \times \frac{1}{cl} \log \frac{I_0}{I} \times \Delta\upsilon_{1/2} \qquad (2)$$

where c is the molar concentration of the absorbing ion per unit volume, I is the optical path length, $\log I_0/I$ is optical density and $\Delta\upsilon_{1/2}$ is half band width.

3.2. Judd-Ofelt Intensity Parameters

According to Judd [21] and Ofelt [22] theory, independently derived expression for the oscillator strength of the induced forced electric dipole transitions between an initial J manifold $|4f^N (S, L) J\rangle$ level and the terminal J' manifold $|4f^N (S',L') J'\rangle$ is given by:

$$\frac{8\Pi^2 mc\bar{\upsilon}}{3h(2J+1)} \frac{1}{n}\left[\frac{(n^2+2)^2}{9}\right] \times S(J, J') \qquad (3)$$

Where, the line strength S (J, J') is given by the equation

$$S(J, J') = e^2 \sum_{\lambda=2,4,6} \Omega_\lambda \langle 4f^N (S, L) J \| U^{(\lambda)} \| 4f^N (S', L') J' \rangle^2 \qquad (4)$$

In the above equation m is the mass of an electron, c is the velocity of light, ν is the wave number of the transition, h is Planck's constant, n is the refractive index, J and J' are the total angular momentum of the initial and final level respectively, Ω_λ (λ=2,4and 6) are known as Judd-Ofelt intensity.

3.3 Radiative Properties

The Ω_λ parameters obtained using the absorption spectral results have been used to predict radiative properties such as spontaneous emission probability (A) and radiative life time (τ_R), and laser parameters like fluorescence branching ratio (β_R) and stimulated emission cross section (σ_p).

The spontaneous emission probability from initial manifold $|4f^N (S', L') J'\rangle$ to a final manifold $|4f^N (S, L) J\rangle$ is given by:

$$A[(S', L') J'; (S, L) J] = \frac{64\pi^2\nu^3}{3h(2J'+1)}\left[\frac{n(n^2+2)^2}{9}\right] \times S(J', J) \qquad (5)$$

Where, $S(J', J) = e^2 [\Omega_2 \| U^{(2)} \|^2 + \Omega_4 \| U^{(4)} \|^2 + \Omega_6 \| U^{(6)} \|^2]$

The fluorescence branching ratio for the transitions originating from a specific initial manifold $|4f^N (S', L') J'>$ to a final many fold $|4f^N (S, L) J >$ is given by

$$\beta [(S', L') J'; (S, L) J] = \sum_{S L J} \frac{A[(S' L)]}{A[(S' L') J' (\bar{S} \bar{L})]} \quad (6)$$

where, the sum is over all terminal manifolds.

The radiative life time is given by

$$\tau_{rad} = \sum_{S L J} A[(S', L') J'; (S, L)] = A_{Total}^{-1} \quad (7)$$

where, the sum is over all possible terminal manifolds. The stimulated emission cross -section for a transition from an initial manifold $|4f^N (S', L') J'>$ to a final manifold $|4f^N (S, L) J >|$ is expressed as

$$\sigma_p(\lambda_p) = \left[\frac{\lambda_p^4}{8\pi c n^2 \Delta\lambda_{eff}}\right] \times A[(S', L') J'; (\bar{S}, \bar{L})\bar{J}] \quad (8)$$

where, λ_p the peak fluorescence wavelength of the emission band and $\Delta\lambda_{eff}$ is the effective fluorescence line width.

3.4 Nephelauxetic Ratio (β') and Bonding Parameter ($b^{1/2}$)

The nature of the R-O bond is known by the Nephelauxetic Ratio (β') and Bonding Parameters ($b^{1/2}$), which are computed by using following formulae [23, 24]. The Nephelauxetic Ratio is given by

$$\beta' = \frac{\nu_g}{\nu_a} \quad (9)$$

where, ν_a and ν_g refer to the energies of the corresponding transition in the glass and free ion, respectively. The value of bonding parameter ($b^{1/2}$) is given by

$$b^{1/2} = \left[\frac{1-\beta'}{2}\right]^{1/2} \quad (10)$$

IV. Result and Discussion

4.1 XRD Measurement

Figure 1 presents the XRD pattern of the sample contain – P_2O_5 which is show no sharp Bragg's peak, but only a broad diffuse hump around low angle region. This is the clear indication of amorphous nature within the resolution limit of XRD instrument.

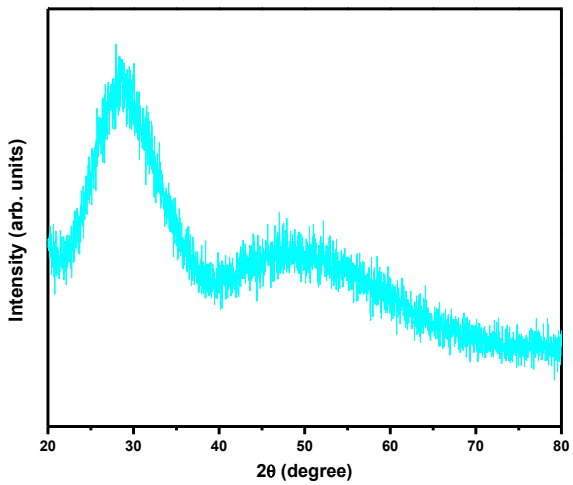

Fig. 1: X-ray diffraction pattern of YZLSLMP HO (1.0) glass.

4.2 Thermal Property

Differential thermal analysis checks the heat absorbed by glass samples during heating or cooling. Fig. 2 depicts the DTA thermogram of powdered YZLSLMP sample. The glass transition temperature (T_g), onset crystallization temperature (T_c), crystallization temperature (T_p), melting temperature(T_m), thermal stability (T_s),Balaji Parameter (B_P), Hurbe's criterion (H_R) and reduced glass transition temperature (T_{rg}) were calculated. Shankar's parameter (K_S) also calculated by using eq. (15). All the determined thermal parameters are given in table 2.

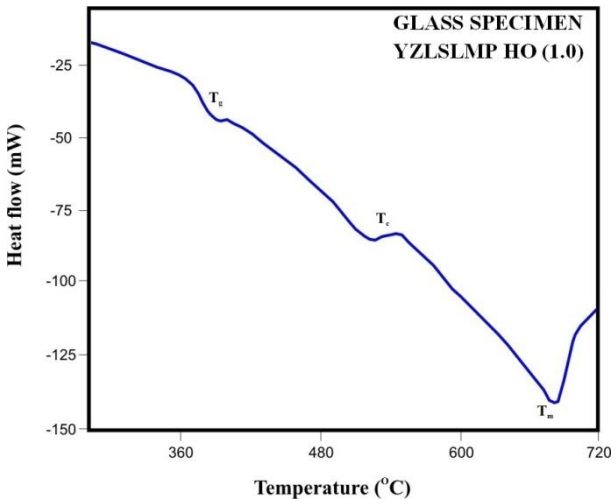

Fig.2: DTA curve of YZLSLMP HO (1.0) glass.

Table 2. Thermal parameters determined from the DTA traces of YZLSLMP HO glasses.

Sample Name	T_g(^{0}C)	T_c(^{0}C)	T_p(^{0}C)	T_m(^{0}C)	T_s(^{0}C)	B_P(^{0}C)	H_R(^{0}C)	K_S(^{0}C)	T_{rg}(^{0}C)
YZLSLMP HO (1.0)	376	510	548	685	134	3.526	0.217	34.234	0.549
YZLSLMP HO (1.5)	380	512	552	688	132	3.300	0.227	33.767	0.552
YZLSLMP HO (2.0)	386	513	555	693	127	3.024	0.233	32.988	0.557

The thermal stability of the glass samples can be calculated by difference between onset crystallization temperature and transition temperature [25].

Thermal stability (T_s) =T_c-T_g (11)

Balaji Parameter can be calculated using [25].

Balaji Parameter (B_P) = [(T_c-T_g)/(T_p-T_c)] (12)

Hruby's criterion is calculated using the Hurby's relation [25].

Hruby's criterion (H_R) = [(T_p-T_c)/(T_m-T_c)] (13)

Reduced glass transition temperature is given as [25].

Reduced glass transition temperature (T_{rg}) =T_g/T_m (14)

Thermal Parameter is given as [25].

K_S= [(T_m-T_c) (T_c-T_g)/T_m] (15)

4.3 Absorption Spectrum

The absorption spectrum of Ho^{3+}doped YZLSLMP glass specimen has been presented in Figure 3 in terms of Intensity versus wavelength. Twelve absorption bands have been observed from the ground state $^5I_8$ to excited states $^5I_5$, $^5I_4$, $^5F_5$, $^5F_4$, $^5F_3$, $^3K_8$, $^5G_6$, $(^5G,^3G)_5$, $^5G_4$, $^5G_2$, $^5G_3$, and$^3F_4$ for Ho^{3+} doped YZLSLMP HO(1.0)glass.

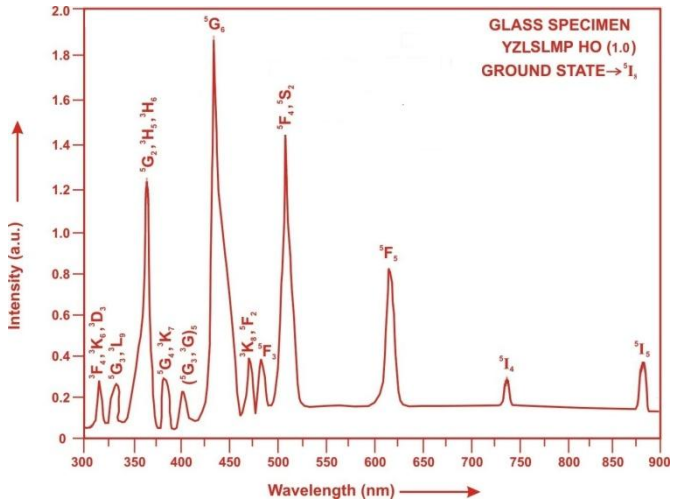

Fig. 3: Absorption spectrum of YZLSLMP HO (1.0) glass.

The experimental and calculated oscillator strength for Ho^{3+} ions in YZLSLMP glasses are given in **Table 3.**

Table 3: Measured and calculated oscillator strength ($P_m \times 10^{+6}$) of Ho^{3+}ions in YZLSLMP glasses.

Energy level from $^5I_8$	Glass YZLSLMP HO(1.0)		Glass YZLSLMP HO(1.5)		Glass YZLSLMP HO(2.0)	
	$P_{exp.}$	$P_{cal.}$	$P_{exp.}$	$P_{cal.}$	$P_{exp.}$	$P_{cal.}$
$^5I_5$	0.52	0.25	0.49	0.25	0.46	0.24
$^5I_4$	0.09	0.02	0.07	0.02	0.06	0.02
$^5F_5$	3.80	2.85	3.76	2.83	3.72	2.79
$^5F_4$	4.78	4.43	4.75	4.40	4.71	4.36
$^5F_3$	1.58	2.47	1.55	2.45	1.51	2.43
$^3K_8$	1.45	2.03	1.42	2.01	1.38	1.97
$^5G_6$	26.66	26.61	25.45	24.42	24.26	24.25
$(^5G,^3G)_5$	3.85	1.72	3.81	1.69	3.77	1.66
$^5G_4$	0.09	0.63	0.07	0.62	0.05	0.61
$^5G_2$	5.98	5.64	5.94	5.43	5.90	5.21
$^5G_3$	1.59	1.44	1.56	1.41	1.52	1.38
$^3F_4$	1.40	4.23	1.37	4.18	1.32	4.11
r.m.s. deviation	±1.1267		±1.1245		±1.1282	

Computed values of F_2, Lande′ parameter (ξ_{4f}**),** Nephlauxetic ratio (β') and bonding parameter ($b^{1/2}$) for Ho^{3+} ions in YZLSLMP glass specimen are given in Table 4.

Table 4: F_2, $\xi_{4f,}$ β' and $b^{1/2}$ parameters for Holmium doped glass specimen.

Glass Specimen	F_2	ξ_{4f}	β'	$b^{1/2}$
Ho^{3+}	358.82	1258.16	0.9337	0.1821

The values of Judd-Ofelt intensity parameters are given in **Table 4.**

Table 5: Judd-Ofelt intensity parameters for Ho^{3+} doped YZLSLMP glass specimens.

Glass Specimen	Ω_2(pm^2)	Ω_4(pm^2)	Ω_6(pm^2)	Ω_4/Ω_6	Ω_λ Tendency	Ref.
YZLSLMP HO (1.0)	6.575	1.368	2.263	0.6045	$\Omega_2 > \Omega_6 > \Omega_4$	P.W.

YZLSLMP HO (1.5)	6.231	1.348	2.248	0.5996	$\Omega_2 > \Omega_6 > \Omega_4$	P.W.
YZLSLMP HO (2.0)	5.897	1.323	2.227	0.5941	$\Omega_2 > \Omega_6 > \Omega_4$	P.W.
LLF (HO)	2.430	1.670	1.840	0.9076	$\Omega_2 > \Omega_6 > \Omega_4$	[26]
PG (HO)	1.930	1.350	1.640	0.8232	$\Omega_2 > \Omega_6 > \Omega_4$	[27]
YZLSLABS (DY)	3.948	1.027	2.689	0.3819	$\Omega_2 > \Omega_6 > \Omega_4$	[28]
BTNMES(ER)	3.530	1.180	2.060	0.5728	$\Omega_2 > \Omega_6 > \Omega_4$	[29]
TLF (ND)	5.610	4.170	5.440	0.7665	$\Omega_2 > \Omega_6 > \Omega_4$	[30]

4.4 Excitation Spectrum

The Excitation spectrum of YZLSLMP (HO 01) glass has been presented in Figure 4 in terms of Excitation Intensity versus wavelength. The excitation spectrum was recorded in the spectral region 325–525 nm fluorescence at 545nm having different excitation band centered at 349,419, 452, 473and 486 nm are attributed to the $^5G_3$, $(^5G, {}^3G)_5$, $^5G_6$, $^3K_8$ and $^5F_3$ transitions, respectively. The highest absorption level is $^5G_6$ and is at 452nm.So this is to be chosen for excitation wavelength.

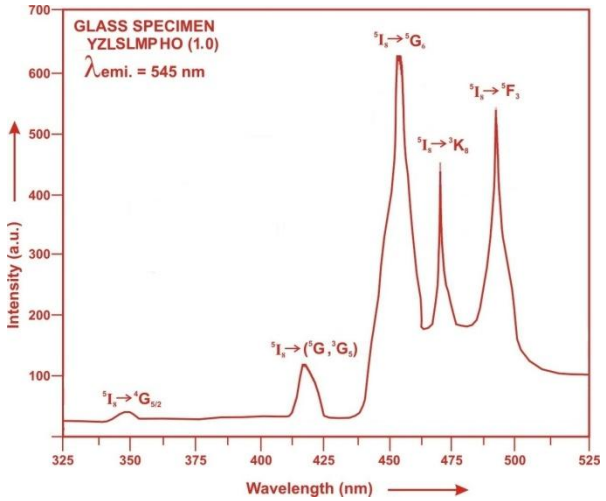

Fig. 4: Excitation spectrum of YZLSLMP HO (1.0) glass.

4.5 Fluorescence Spectrum

The fluorescence spectrum of Ho^{3+}doped in ytterium zinc lithium sodalime magnesium phosphate glass is shown in Figure 5. There are eleven broad bands observed in the Fluorescence spectrum of Ho^{3+}doped ytterium zinc lithium sodalime magnesium phosphate glass. The wavelengths of these bands along with their assignments are given in Table 6. The peak with maximum emission intensity appears at 2035 nm and corresponds to the $(^5I_7 \rightarrow {}^5I_8)$ transition.

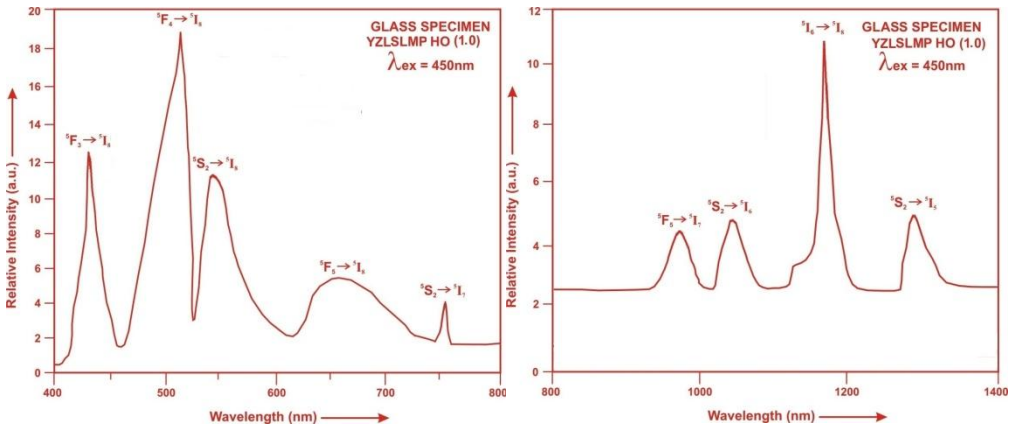

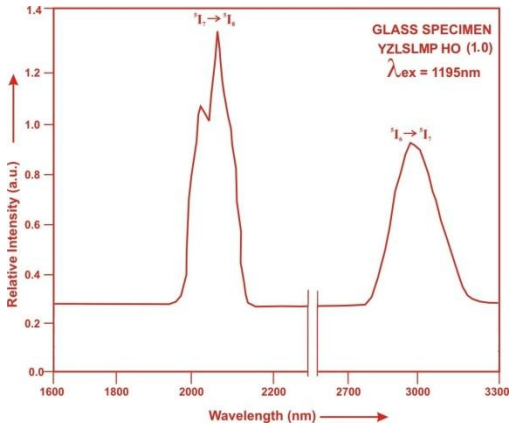

Fig. 5: Fluorescence spectrum of YZLSLMP HO (1.0) glass.

Table6: Emission peak wave lengths (λ_p),radiative transition probability (A_{rad}),branching ratio (β),stimulated emission cross-section(σ_p) and radiative life time(τ_R) for various transitions in Ho^{3+} doped YZLSLMP glasses.

Transition		YZLSLMP HO(1.0)				YZLSLMP HO(1.5)				YZLSLMP HO(2.0)			
	λ_{max} (nm)	$A_{rad}(s^{-1})$	β	σ_p (10^{-20} cm^2)	$\tau_R(\mu s)$	$A_{rad}(s^{-1})$	β	σ_p (10^{-20} cm^2)	τ_R (μs)	$A_{rad}(s^{-1})$	β	σ_p (10^{-20} cm^2)	τ_R (10^{-20} cm^2)
$^5F_3 \rightarrow {}^5I_8$	435	4237.66	0.2487	0.574		4217.96	0.2489	0.557		4186.88	0.2491	0.536	
$^5F_4 \rightarrow {}^5I_8$	501	6717.03	0.3942	1.220		6678.60	0.3941	1.183		6621.19	0.3940	1.137	
$^5S_2 \rightarrow {}^5I_8$	555	1768.85	0.1038	0.446		1760.63	0.1039	0.436		1747.66	0.1040	0.421	
$^5F_5 \rightarrow {}^5I_8$	652	1908.78	0.1120	0.735		1895.15	0.1118	0.719		1875.78	0.1116	0.698	
$^5S_2 \rightarrow {}^5I_7$	761	1341.90	0.0787	1.108	5867.99	1335.67	0.0788	1.085	5900.82	1325.83	0.0789	1.033	5950.72
$^5F_5 \rightarrow {}^5I_7$	995	446.38	0.0262	1.203		441.58	0.0261	1.161		435.60	0.0259	1.125	
$^5I_6 \rightarrow {}^5I_8$	1032	205.62	0.0121	0.698		204.51	0.0121	0.681		202.84	0.0121	0.662	
$^5S_2 \rightarrow {}^5I_5$	1195	235.38	0.0138	1.214		233.86	0.0138	1.185		231.73	0.0138	1.149	
$^5S_2 \rightarrow {}^5I_6$	1310	62.67	0.0037	0.615		62.37	0.0037	0.594		61.89	0.0037	0.577	
$^5I_7 \rightarrow {}^5I_8$	2035	93.49	0.0055	4.623		92.84	0.0055	4.476		91.94	0.0055	4.350	
$^5I_6 \rightarrow {}^5I_7$	2925	23.85	0.0014	3.969		23.63	0.0014	3.854		23.36	0.0014	3.752	

V. Conclusion

In the present study, the glass samples of composition $(45\text{-}x)P_2O_5$: 10ZnO: $10Li_2O$: $10Na_2O$: 15CaO: 10MgO: $10Y_2O_3$:xHo_2O_3 (where x =1, 1.5and 2mol %) have been prepared by melt-quenching method. The value of stimulated emission cross-section (σ_p) is found to be maximum for the transition ($^5I_7 \rightarrow {}^5I_8$) for glass YZLSLMP HO (1.0), suggesting that glass YZLSLMP HO (1.0) is better compared to the other two glass systems YZLSLMP HO(1.5) and YZLSLMP HO(2.0). The large value of Balaji and Shankar parameters indicate that the prepared glass samples have good thermal stability. The large stimulated emission cross section in borate glasses suggests the possibility of utilizing these systems as laser materials. The results show that the Ho^{3+} doped phosphate glasses could be potential candidates for 2.0μm optoelectronic applications.

References

[1]. Meena, S.L. (2025). Spectral and Thermal properties of Eu^{3+} doped Ytterium Zinc Lithium Alumina Tungsten Potassiumniobate Bismuth Borate Glasses with low Hruby's criterion, IOSR Appl.Phys.17,48-54.

[2]. Arora,R.,Kaur,N.,Singh,H.,Kumar,D.,Bhatia,V.,Singh,S.P.(2024).B_2O_3-TeO_2-ZnO-Na_2O-Nd_2O_3 glass matrices: A comprehensive study of physical,structural,optical and thermoluminescence properties,Mater.Chem.Phys.313,128783.

[3]. Meena, S.L. (2022). Spectral and Up conversion Properties of Dy^{3+} ions doped Zinc Lithium Potessiumniobate Borosilicate Glasses,Int.Eng.Sci.Inv.11, 44-49.

[4]. Prabhu,N.S.,Hegde,V.,Wagh,A.,Sayyed,M.I.,Agar,O.,Kamath,S.D.(2019).Physical,structural and optical properties of Sm^{3+} doped lithium zinc alumino borate glasses,J.Non-Cryst.Solids,515,116-124.

[5]. Matos,I.M.,Balzaretti, N.M.(2024).Effect of mixed alkali ions on the structural and spectroscopic properties of Nd^{3+} doped silicate glasses,Res.Mat.21,100517,1-8.

[6]. Shaari,H.R.,Azian,M.N.,Azlina,Y.,Hajer,S.S.,Nazrin,S.N.,Umer,S.A.,Kenzhaliyev,B.K.,Boukhris,I.,AlHada,N.M.(2021).Investigation of Structural and Optical Properties of Graphene Oxide-Coated Neodymium Nanoparticles Doped Zinc-Tellurite Glass for Glass Fiber,J.Ino.Org.Poly.Mat.10904-021-02061-7.

[7]. Barik,S.K.,Senapati,A.,Chkaraborty,S.,Ananthasivan,K.(2023).Structure and Optical Properties of Sodium Alumino Phosphate Glass Matrix Containing Lanthanide Oxides (Ce,Pr,Nd and Gd), J.Ino.Org.Poly.Mat.33:2093-2110.

[8]. Singh,H.,Singh,D.,Singh,S.P.(2025).Er^{3+},Nd^{3+},Tm^{3+}:Up-conversion in Lead Borophosphate Glasses for Visible Emission,J.Flu.35,5145-5157.

[9]. Meena,S.L.(2020).Thermal and Physical Properties of Tm^{3+} ions doped Lead Lithium Borophosphate Glasses, IOSR Appl.Phys.12,27-33.

[10]. Madhu,A.,Eraiah,B.,Manasa,P.,Basavapoornima, Ch.(2018).Er^{3+} ions doped lithium-bismuth boro phosphate glass for 1532 nm emission and efficient red emission up conversion for telecommunication and lasing application,J.Non-Cryst.Solids,495,35-46.

[11]. Mahraz,Z.A.S.,Sazali,E.,Sahar,M.,Amran,N.U.,Yaacob,S.,Aziz,S.M.,Mawlud,S.,Noor,F.,Harun,A.(2019).Spectroscopic inestigations of near-infrared emission from Nd^{3+} doped zinc phosphate glasses, Judd-Ofelt evaluation,J.Non-Cryst.Solids,509,106-114.

[12]. Zhang,L.,Xia,Y.,Shen,X.,Wei,W.(2019).Concentration dependence of visible luminescence from Pr^{3+} doped phosphate glasses, Spectrochim, Acta A,206,454-459.

[13]. Basavapoornima,C.,Kesavulu,C.R.,Maheswari,T.,Pecharapa,W.,Depuru,S.R.,Jayasankar,C.K.(2020).Spectral characteristics of Pr^{3+} doped lead based phosphate glasses for optical display device applications.J.Lumin.228,117585.

[14]. Han,X.,Shen,L.,Pun,E.Y.B.,Ma,T.,Lin,H.(2014).Pr^{3+} doped phosphate glasses for fiber amplifiers operating at 1.38-1.53μm of the fifth optical telecommunication window,Opt.Mater.36,1203-1208.

[15]. Kilic,G.,Ilik,E.,Mahmoud,K.A.,Mallawany,R.El,Agawany,El(2020).Novel zinc vanadyl borophosphate glasses:ZnO-V_2O_5-P_2O_5-B_2O_3:Physical,thermal and nuclear radiation shielding properties,Ceram.Int.46,19318-19327.

[16]. Selvi,S.,Marimuthu,K.,Muralidharan,G.(2015).Structural and luminescence behavior of Sm^{3+} ions doped lead- boro- telluro-phosphate glasses,J.Lumin.159,207-218.

[17]. Meena,S.L.(2020).Spectroscopic Properties of Nd^{3+} doped Lead Lithium Sodium Tungsten Borophosphate Glasses,Int.J.Chem.Phy.Sci.9,11-18.

[18]. Taherunnisa,S.,Rudramamba,K.S.,Krishna Reddy, D.V., Venkateswariu,T., Zhydachevskyy,Y., Suchochi,A.,Piasecki,M.,RamiReddy,M.(2020).Efficient 2.01μm mid-infrared(MIR) and visible emission in Ho^{3+} doped phosphate glasses enhanced by Er^{3+} ions,Infr.Phys.Techn.107,103294.

[19]. Meena,S.L.(2025).Spectral and Raman Analysis of Tb^{3+} doped Yttrium Zinc Lithium Ceasium Barium Borate Glasses,IOSR Appl.Phys.17,41-47.

[20]. Meena,S.L.(2021).Spectral and Raman Analysis of Sm^{3+} doped in Zinc Lithium Sodalime Alumino Silicate Glasses,Int.J.Eng.Sci.Inven.10,28-33.

[21]. Judd,B.R.(1962).Optical absorption intensities of rare-earth ions,Phys.Resv.127,750-761.

[22]. Ofelt,G.S.(1962).Intensities of crystal spectra of rare-earth ions,J.Chem.Phys.37,511-520.

[23]. Kashif,I.Ratep,A.(2023).Luminescence in Er^{3+} co-doped bismuth germinate glass-ceramics for blue and green emitting applications,J.Korean Ceram.Soc.60,511-526.

[24]. Meena,S.L.(2021).Spectral and Raman Analysis of Er^{3+} doped Zinc Lithium Antimony Sodalime Tellurite Glasses,Int.J.Eng.Sci.Inv.10,09-15.

[25]. Meena,S.L.(2026). Structural, Thermal and Photoluminescence Analysis of Pr^{3+} Doped Borophosphate Glasses for the Visible Light Emitting Diodes Applications, IOSR Appl.Phys.18,55-62.

[26]. Nachimuthu,P.,Jagannathan,R.(1999).Judd-Ofelt Parameters,Hypersensitivity and Emission Characteristics of Ln^{3+}(Nd^{3+},Ho^{3+} and Er^{3+})Ions Doped in PbO-PbF_2 Glasses,J.Am.Ceram.Soc.82(2),387-92.

[27]. Liu,P.,Han,C.,Zhang,X.,Li,X.,Wan,Y.,Zhang,H.,Su,C.(2024).Synthesis and upconversion luminescence of Ho^{3+}-Yb^{3+} co-doped glass ceramics containing $LiGd(WO_4)_2$,Ceram.Int.50(17),31164-31172.

[28]. Meena,S.L.(2025).Spectral, Thermal and Raman Analysis of Dy^{3+} Doped Borosilicate Glasses with Large Thermal Stability Parameter,Int.Eng.Sci.Inv.14,11-18.

[29]. Radin, N.L.A.,Sahar,M.(2018).Erbium doped sodium magnesium boro-tellurite glass: Stability and Judd-Ofelt analysis. Matter.Chem.Phys.216,177-185.

[30]. Kumar,V.R.K.,Bhatnagar,A.K.,Jagannathan,R.(2001).Structural and optical studies of Pr^{3+},Nd^{3+},Er^{3+} and Eu^{3+} ions in tellurite based oxyfluoride,TeO_2-LiF glass, J.Phys.D Appl. Phys.34,1563.